Materials Chemistry and Physics 141 (2013) 920–928

Contents lists available at SciVerse ScienceDirect

Materials Chemistry and Physics

journal homepage: www.elsevier.com/locate/matchemphys

Significant improvement in the thermoelectric properties of zwitterionic polysquaraine composite films

Mei-Chan Ho [a], Ching-Hsun Chao [b], An-Ya Lo [c,*], Chun-Hua Chen [a], Ren-Jye Wu [d], Mei-Hui Tsai [e], Yi-Chia Huang [a], Wha-Tzong Whang [a,*]

[a] Department of Materials Science and Engineering, National Chiao Tung University, 1001 Ta-Hsueh Road, Hsin-Chu 30010, Taiwan R.O.C
[b] Dow Chemicals, Advanced Materials, Electronic Materials, No. 6, Kesi 2nd Road, Jhunan, Miaoli, Science-Based Industrial Park 35053, Taiwan R.O.C
[c] Department of Materials Science and Engineering, Green Energy Development Center, Feng Chia University, No. 100, Wenhwa Road, Seatwen, Taichung 40724, Taiwan R.O.C
[d] Industrial Technology Research Institute, Material and Chemical Research Laboratories, Rm 104, Bldg 67, 195, Sec. 4, Chung Hsing Road, Chutung, Hsinchu 31040, Taiwan R.O.C
[e] Department of Chemical and Materials Engineering, National Chin-Yi University of Technology, No. 57, Sec. 2, Zhongshan Road, Taiping, Taichung 41170, Taiwan R.O.C

HIGHLIGHTS

- Polysquaraine $SQI_{0.1}$ blended with SWNTs and CMK-3 can develop freestanding film.
- SWNTs well-dispersed in the $SQI_{0.1}$ matrix and endowed the composite with flexibility.
- The iodine-doped $SQI_{0.1}$-based films have potential for thermoelectric application.
- Thermoelectric efficiency of composite can be promoted by SWNTs and CMK-3.

GRAPHICAL ABSTRACT

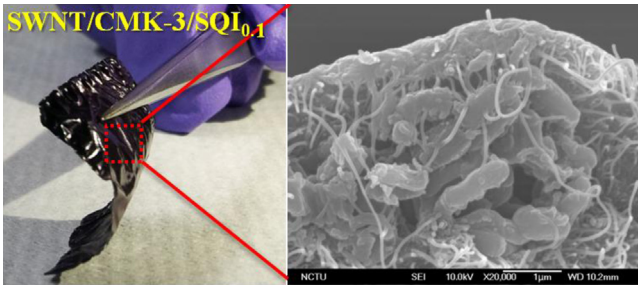

ARTICLE INFO

Article history:
Received 18 February 2013
Received in revised form
21 June 2013
Accepted 22 June 2013

Keywords:
Polymer
Composite materials
Electrical conductivity
Thermoelectric effects

ABSTRACT

In this study, the polysquaraine $SQI_{0.1}$, a zwitterionic π-conjugated polymer, was adopted as the matrix for the preparation of flexible and freestanding films; the low band gap of this semiconducting polymer made it a natural choice for use as a thermoelectric (TE) polymer. To enhance their TE applications, both single-walled carbon nanotubes (SWNTs) and mesoporous carbon (*i.e.*, CMK-3) were integrated into the $SQI_{0.1}$-based films and the effects of doping with iodine were also investigated. Using scanning electron microscopy, the variations in morphology of these $SQI_{0.1}$-based films were examined. Raman spectroscopy was used to study the π−π interactions between iodine and the carbon materials (*i.e.*, SWNT, CMK-3); X-ray diffraction and Raman spectroscopy to investigate the intercalation of the doped iodine in the composite films; and X-ray photoelectron spectroscopy to determine the valence state of the doped iodine. The TE properties of these materials were characterized in terms of the electrical conductivity (σ), thermal conductivity (κ), and Seebeck coefficient (S). The TE properties of the iodine-doped composite film prepared from SWNTs, CMK-3, and $SQI_{0.1}$ included a notable value of ZT (Figure of Merit) of 4.563×10^{-3}, which was 143% of that of the corresponding iodine-doped $SQI_{0.1}$ film.

* Corresponding authors.
E-mail addresses: a.y.lo1125@gmail.com (A.-Y. Lo), wtwhang@mail.nctu.edu.tw (W.-T. Whang).

0254-0584/$ – see front matter © 2013 Elsevier B.V. All rights reserved.
http://dx.doi.org/10.1016/j.matchemphys.2013.06.024

1. Introduction

Because of their niche applications (*e.g.*, wearable electronics), polymer-based thermoelectric (TE) materials have attracted widespread research attention. Although traditional π-conjugated polymers are excellent choices for TE applications because of their intrinsic semiconductivities [1–4], their low electrical conductivities and low Seebeck coefficients lead to small TE figures of merit—for example, a low efficiency index of TE converters ($ZT = S^2\sigma T/\kappa$; where S, σ, T, and κ are the Seebeck coefficient, electrical conductivity, absolute temperature, and thermal conductivity, respectively).

This problem can potentially be solved by polysquaraine, a zwitterionic π-conjugated polymer, because the band gap energy can be decreased effectively and strong charge-transfer interactions can be induced by its alternating donor/acceptor repeating units and resonance-stabilized zwitterionic structure [5–7]. To the best of our knowledge, however, no freestanding zwitterionic π-conjugated polymers have been prepared, restricting their use in TE applications. Gratifyingly, this limitation can be overcome by using the ionic liquid (IL)–coordinating method that we have proposed previously [8], which is crucial to broaden its applications in solar cells [9,10], optical data storage [11], and NIR Photography [12]. Other than optoelectronic applications, it is worth to be mentioned that freestanding zwitterionic π-conjugated polymers film would create great potential on TE applications due to its intrinsic electrical conductivity, good thermal stability, and low thermal conductivity.

Another approach that has been adopted widely to enhance the values of σ of conjugated polymers has been doping with suitable agents [13–16]. Iodine, for example, can greatly improve the values of σ by more than seven orders of magnitude [17]. In addition, carbon nanotubes (CNTs) and mesoporous carbons (*e.g.*, CMK-3) have also been applied widely to enhance the values of σ of polymers because of their own outstanding values of σ and mechanical properties [14,18]. In addition, CMK-3 is a well-established material for nanoparticle dispersion because of its excellent specific surface area (*ca.* 1000 $m^2\ g^{-1}$), nanoporosity (*ca.* 3 nm), and specific pore volume (*ca.* 1 cc g^{-1}) [19]. Nevertheless, the potential of these materials for dispersing doping agents has been overlooked until now.

In this study, CMK-3 was adopted to enhance the value of σ and, especially, the porosity for the separation of iodine in freestanding $SQI_{0.1}$ films; single-walled carbon nanotubes (SWNTs) were also integrated into freestanding $SQI_{0.1}$ films to enhance the values of σ and the flexibility. Thorough investigation was carried out on the morphologies, properties, and their interrelationships. As the

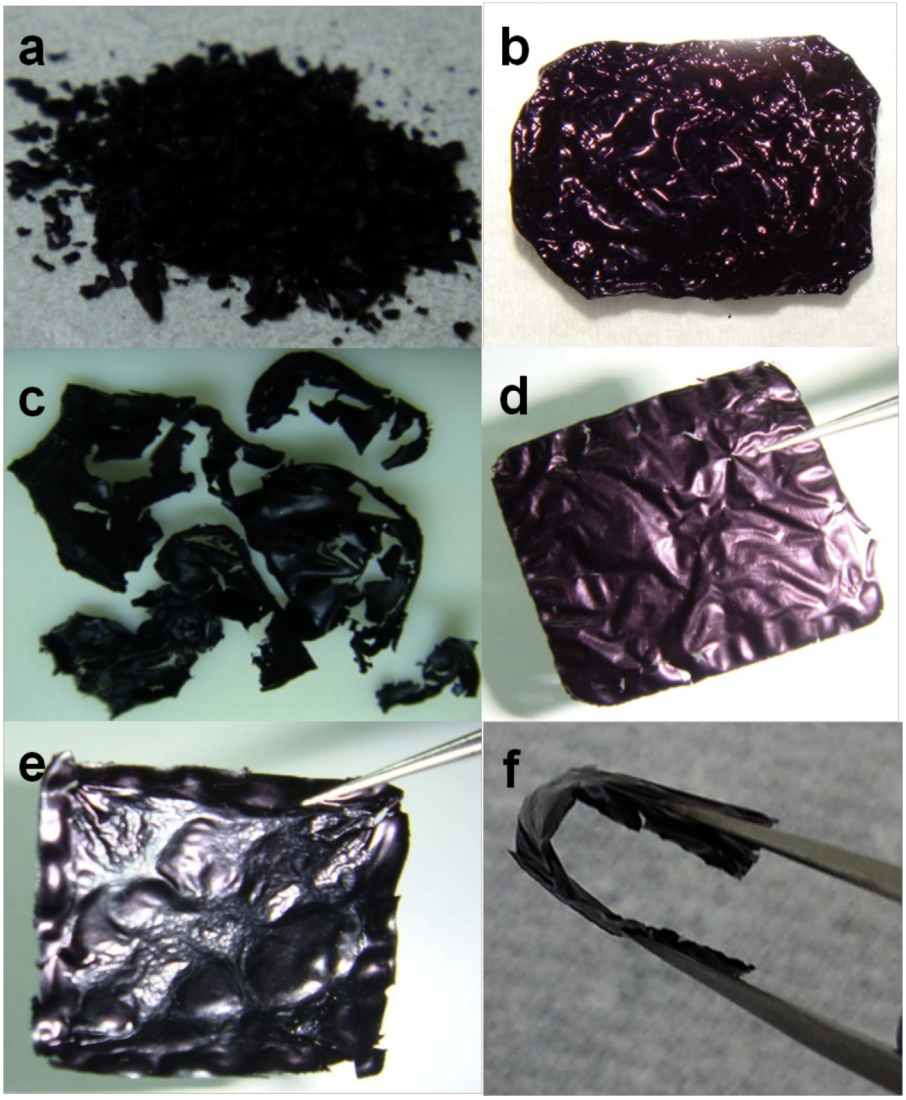

Fig. 1. Photographs of specimens: (a) SQ powder, (b) $SQI_{0.1}$, (c) 5CMK/$SQI_{0.1}$, (d) 20NT/$SQI_{0.1}$, and (e, f) 20NT/5CMK/$SQI_{0.1}$.

result, the $SQI_{0.1}$-based composite films exhibiting good thermoelectrical and mechanical properties can be obtained. Further study on structure design of composite films would probably improve the conductivity again [20].

2. Experimental section

2.1. Poly(bispyrrole-co-squaric acid) (SQ)

2,5-Bis(dodecyloxy)-1,4-dibenzyl phosphonate (BDCBP) was synthesized from 2,5-bis(dodecyloxy)-1,4-bis(bromomethyl)benzene and triethyl phosphate (97%, Sigma–Aldrich) following a previously reported procedure [21]. Desired amounts of BDCBP, squaric acid (99%, Acros), butanol, and benzene were then heated under reflux at 120 °C for 24 h, yielding polysquaraine from the insoluble precipitated powder. In a previous report [8], the IL methyltrioctylammonium trifluoromethanesulfonate (99%, URMATOATS) was found to play a critical role in the formation of freestanding $SQI_{0.1}$ films. In this study, a solution of $SQI_{0.1}$ containing 0.1 wt% of this IL was used to prepare flexible, freestanding $SQI_{0.1}$-based films.

2.2. SBA-15 mesoporous silica and CMK-3 mesoporous carbon

SBA-15, the template of CMK-3, was prepared following the synthetic procedure reported by Zhao et al. [22]. Typically,

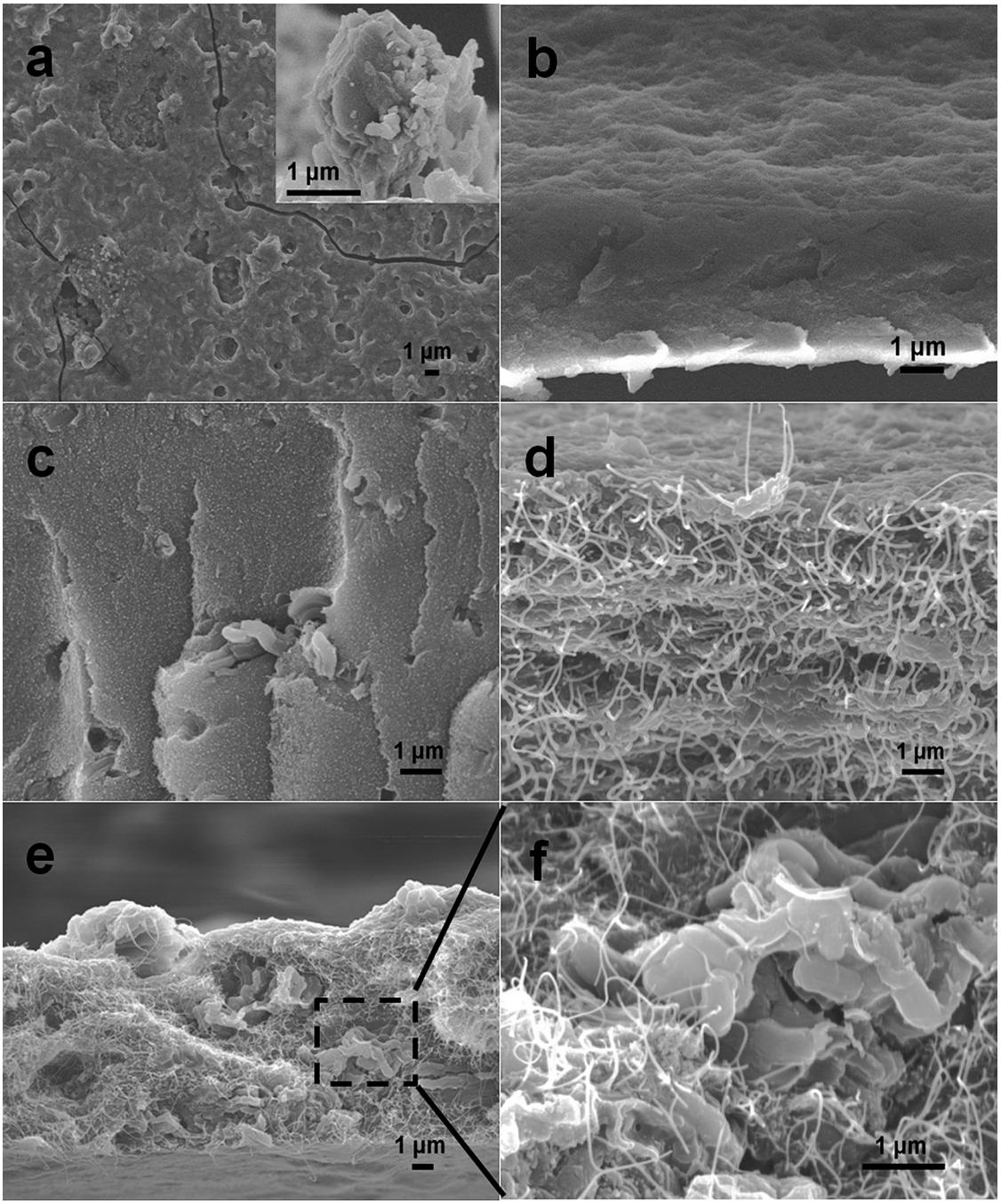

Fig. 2. SEM images of $SQI_{0.1}$-based films: (a) top-view image of SQ film coated on substrate (inset: irregular snipping removed from substrate), the cross-session of (b) $SQI_{0.1}$, (c) 5CMK/$SQI_{0.1}$, (d) 20NT/$SQI_{0.1}$ and (e, f) 20NT/5CMK/$SQI_{0.1}$ composite films.

tetraethyl orthosilicate (TEOS; ≥99%; Sigma–Aldrich), hydrochloric acid (HCl; 37%), and the triblock copolymer P_{123} (PEO_{20}-PPO_{70}-PEO_{20}; M_n = 5800; Sigma–Aldrich) were mixed at a desired ratio, stirred at 40 °C for approximately 2 h, and then aged at 100 °C for 2 days. The solid product was then filtered off, washed with H_2O, and dried at 100 °C prior to calcination in air at 560 °C for 6 h. The resultant SBA-15 was then impregnated with the carbon source [D-(+)-sucrose, 99+%; Acros] following reported procedures [23,24]. A viscous mixture of SBA-15, sucrose, H_2O, and H_2SO_4 (weight ratios: 2:2.5:10:0.28) was ground, dried at 60 °C, and then dehydrated at 160 °C for 6 h; this procedure was repeated once using sucrose (1.6 g), H_2O (6.4 g), and H_2SO_4 (0.18). The obtained mixture was carbonized under Ar at 900 °C for 1 h. After removing SBA-15 through $HF_{(aq)}$ etching, the CMK-3 powder was filtered off and dried.

2.3. Specimen designation and post-treatment through iodine-doping

For the preparation of pristine/composite films, a desired amount of SWNTs (>90 wt.%, Cheap Tubes) or CMK-3 was suspended in the $SQI_{0.1}$ solution through ultrasonication for 4–5 h prior to casting on a glass substrate (2.5 × 2.5 cm^2); after evaporation of the solvent at 80 °C for 2 h, the flexible composite films were flaked off from substrate in MeOH solution and dried under vacuum at 100 °C for 24 h.

The as-synthesized pristine/composite films were further doped with iodine using a previously reported procedure [25, 26]. In short, the pristine/composite films were placed in a sealed jar containing iodine crystals and heated for 2–24 h at 35–50 °C. Finally, the residual iodine vapor was removed under vacuum for 1 h.

2.4. Characterization

Fourier-transform infrared (FTIR) spectra were recorded using a PerkinElmer Spectrum 100 spectrometer. Thermogravimetric analysis (TGA) was performed under N_2 (99.99%) using a Q500 thermogravimetric analyzer operated at a heating rate of 15 °C min^{-1} (from room temperature to 700 °C). Powder X-ray diffraction (XRD) and X-ray photoelectron spectroscopy (XPS) were performed using a Bruker NanoStar SAXS system (Cu Kα radiation) and a Thermo Scientific K-Alpha apparatus, respectively. The electrical conductivities (σ) of the polymers were measured using a four-point probe electrical measurement analyzer (RT-80/RG-80, Napson). For Seebeck coefficient measurements, a microheater was applied to control the temperature difference across the polymer film. Two points along the heat flow direction were selected, and the corresponding temperatures were measured by calibrated thermocouples. The temperature difference (ΔT) between these two points could be derived. The Seebeck voltages (ΔV) were detected via using the data acquisition system (Keithley 2700) through a pair of thin Cu wires connected to the sample at same points as the junctions of thermocouples. The Seebeck coefficient ($S = \Delta V/\Delta T$) could be acquired. The microstructures and morphologies of the specimens were analyzed through transmission electron microscopy (TEM), using a Cryo-HRTEM microscope (JEM-2010), and scanning electron microscopy (SEM), using JSM-6500 and JSM-6700 microscopes. The values of κ of the pristine/composite films were evaluated using the ASTM D5470 process and a CL-TIM-III thermal conductivity measurement instrument (Megtron Technical). Raman spectra were recorded in the range from 100 to 2000 cm^{-1} using a Horiba Jobin-Yvon Raman spectrometer (Ar laser; wavelength: 514.5 nm).

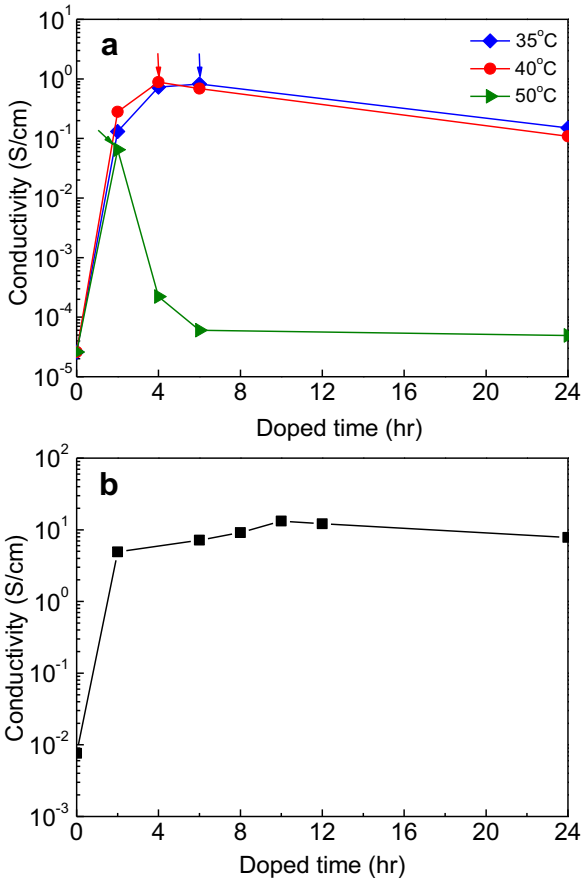

Fig. 3. The variation of electrical conductivity variation versus the iodine-doping conditions of $SQI_{0.1}$-based polymer films: (a) $SQI_{0.1}$ film and (b) 20NT/5CMK/$SQI_{0.1}$ composite film for iodine-doping at 35 °C.

3. Results and discussion

3.1. Evolution and morphology of polysquaraine-based films

The evolution of the freestanding $SQI_{0.1}$-based films is presented in Fig. 1. Synthetic SQ-based polymers have, until recently [8], been prepared only in the form of powders (Fig. 1a) [5], and not in the

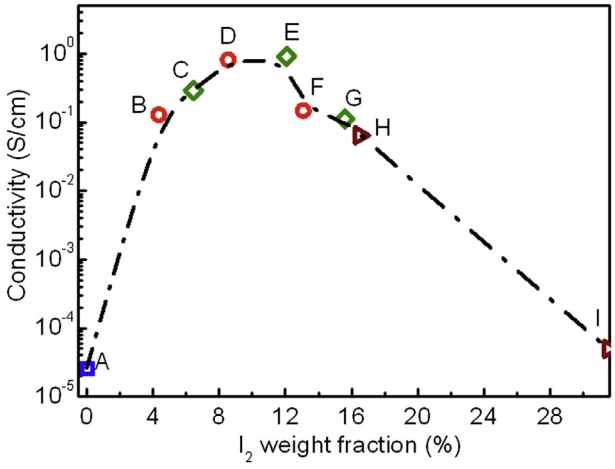

Fig. 4. The variation trend of electrical conductivity versus the iodine mass fraction of $SQI_{0.1}$ films: (□) pristine $SQI_{0.1}$, and doped under 35 °C (○), 40 °C (◇), and 50 °C (△).

form of freestanding films (Fig. 1b). On the other hand, the proposed polysquaraine films exhibited great potential for TE applications, due to the zwitterionic π-conjugated structure and intrinsically low band gap (E_g = 0.8–1.1 eV) [5, 6]. To further improve its potential TE applications, CMK-3 and SWNTs were integrated into $SQI_{0.1}$ films at various ratios in this study. The integration of CMK-3 disrupted film formation, as revealed in Fig. 1c, presumably because of the loose structure that existed after exceeding the critical degree of porosity. In contrast, the integrated SWNTs (20 wt.%) enhanced the formation of freestanding films (Fig. 1d). Therefore, for subsequent film formation, additional SWNTs were applied to overcome the drawbacks of adding CMK-3. The optimal film, formed from 20 wt.% of SWNTs integrated together with 5 wt.% of CMK-3 in the $SQI_{0.1}$ film (denoted as 20NT/5CMK/$SQI_{0.1}$), exhibited metallic luster (Fig. 1e) and good flexibility (Fig. 1f).

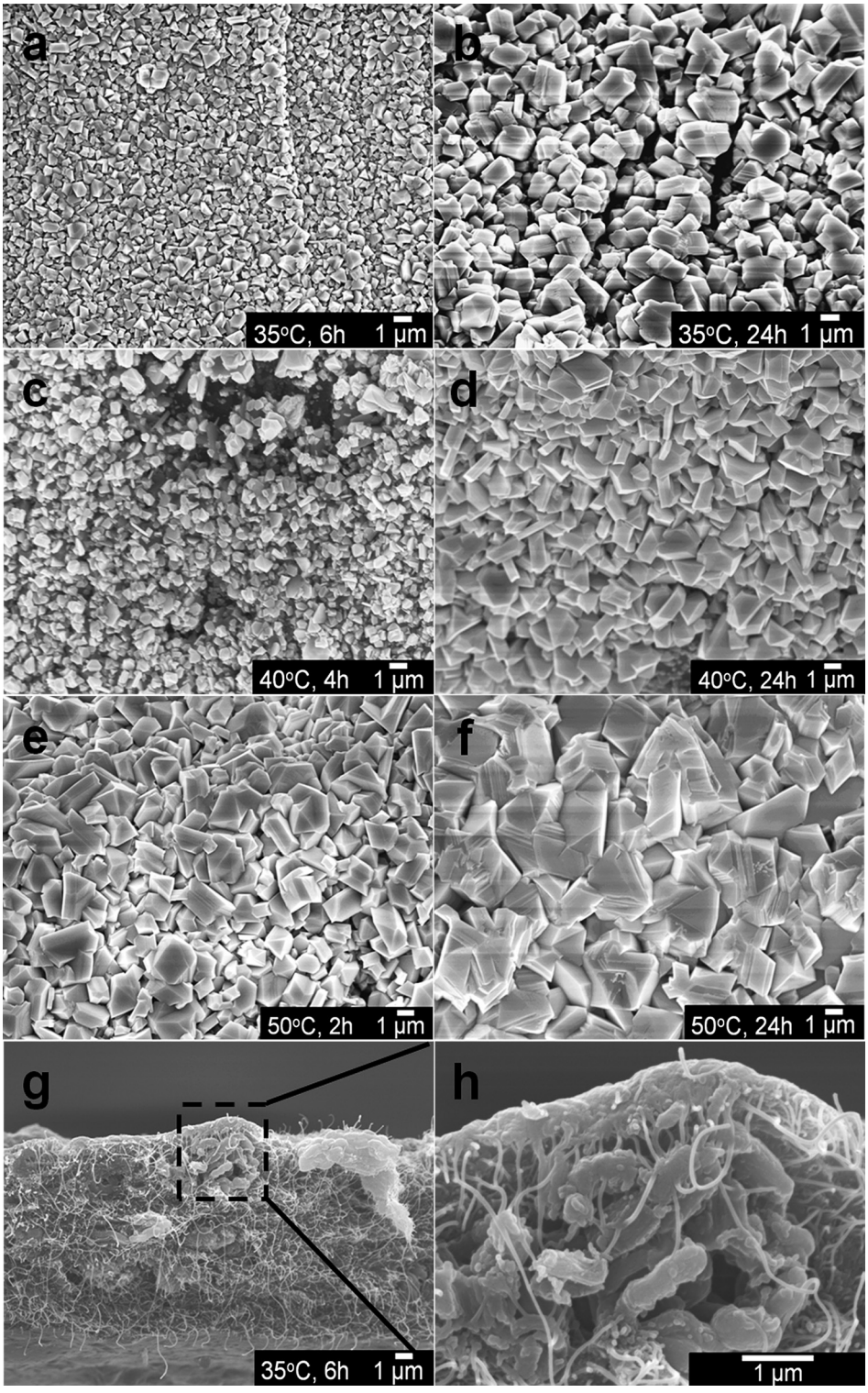

Fig. 5. Cross-section SEM images of iodine-doped (a–f) $SQI_{0.1}$ films, and (g, h) 20NT/5CMK/$SQI_{0.1}$ film.

SEM images of the various materials in Fig. 1 are presented in Fig. 2. A top-view image of the $SQI_{0.1}$ film prior to its removal from the substrate is provided in Fig. 2a; once it had been removed from the substrate, only irregular/disintegrated snipping was obtained (see the inset). After the addition of the IL, the SEM image (Fig. 2b) reveals a rather smooth cross-session, result in a good freestanding film (Fig. 1b). The dispersion of CMK-3 (Fig. 2c) in the $SQI_{0.1}$ film was not as good as that of the CNTs, leading to rather poor flexibility, consistent with Fig. 1c. Although it is well-established that SWNTs tend to entangle with one another, the SWNTs were dispersed well in the polysquaraine matrix, as revealed in Fig. 2d, presumably because of strong π–π interactions between the SWNTs and the π-conjugated electrons of the $SQI_{0.1}$ main chain (*vide infra*: Raman spectroscopic results) [27]. Well-dispersed SWNTs penetrating through the film appear in the cross-section of 20NT/5CMK/$SQI_{0.1}$ (Fig. 2e); the CMK-3 units were bound and fixed by these SWNTs in the $SQI_{0.1}$ matrix (Fig. 2f). Hence, good freestanding films were observed in Fig. 1e and f.

3.2. Effect of iodine-doping on morphology and electrical conductivity (σ) of polysquaraine ($SQI_{0.1}$)-based film

To determine the effects of doping with iodine, the variations in the values of σ of $SQI_{0.1}$ with respect to the doping conditions (35, 40, or 50 °C for 0–24 h) were investigated (Fig. 3a). The value of σ of the iodine-doped $SQI_{0.1}$ film increased rapidly from 2.589×10^{-5} S cm^{-1} to approximately 10^{-1} S cm^{-1} after the doping temperature had been increased from 35 to 50 °C. The highest values of σ for each doping temperature varied depending on the doping time: 8.236×10^{-1} S cm^{-1} after 6 h at 35 °C, 8.816×10^{-1} S cm^{-1} after 4 h at 40 °C, and 6.446×10^{-2} S cm^{-1} after 2 h at 50 °C. The conclusion drawn from these enhanced values was that the charge carriers were incorporated well and positioned along with the π-bond conjugated main chain [28]. According to Zeng et al., over-doping of iodine in π-conjugated polymers would retain the value of σ at the same level [29]. In case of the zwitterionic π-conjugated polymer reported herein, however, excessive amounts of iodine-doping led to decreased values of σ, especially in the cases when doping was performed at temperatures below 50 °C (Fig. 3). This phenomenon has not been described previously; from the viewpoint of zwitterionic π-conjugation, an excessive amount of doped iodine might have provided a greater possibility of attracting the delocalization of negative charge along the backbone of the zwitterionic polymer. Finally, the stability exhibited by the iodine-doped $SQI_{0.1}$ films prepared herein was excellent under ambient conditions, even after exposure to the air for 14 days (Fig. S1). To determine the effect of the mass fraction of iodine, the relationship between the mass fraction of iodine and the value of σ was examined (Fig. 4). The same trend was exhibited by the $SQI_{0.1}$ films that had been doped at different temperatures, with the value of σ having increased when the content of iodine was increased in the initial stage. Optimization of the value of σ (8.816×10^{-1} S cm^{-1}) occurred in the presence of 8–12 wt.% of iodine. As a result, the highest value of σ for the $SQI_{0.1}$ system appeared after doping at 35 °C for 6 h.

The effect of the iodine-doping time on the value of σ for the 20NT/5CMK/$SQI_{0.1}$ composite film system was also examined. The value of σ of 20NT/5CMK/$SQI_{0.1}$ increased dramatically (Fig. 3b) from 7.63×10^{-3} S cm^{-1} to 13.21 S cm^{-1}, thereafter reaching a plateau, when the doping time was increased from 0 to 10 h (35 °C). This value was tenfold higher than that of the iodine-doped $SQI_{0.1}$ film (*cf.* Fig. 3a). The better dispersion of iodine, as had been observed also through SEM analysis, appeared to be responsible for this behavior.

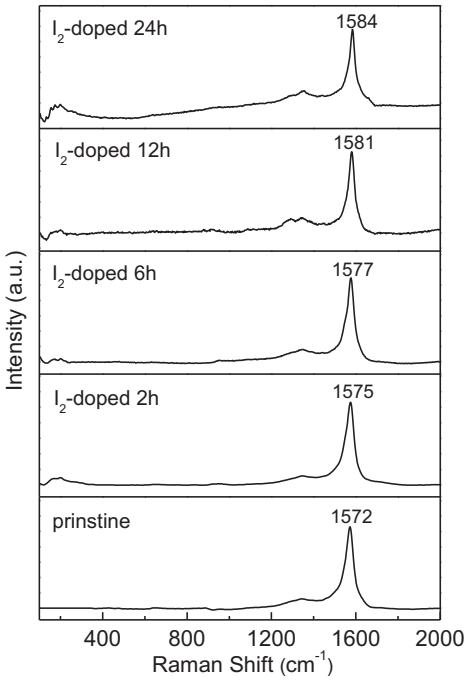

Fig. 6. Raman spectra of 20NT/5CMK/$SQI_{0.1}$ composite films doped under 35 °C for 0–24 h.

To determine the morphological effects of doping with iodine, SEM images of cross-sections of various $SQI_{0.1}$-based films were recorded (Fig. 5). The grains of iodine were small (*ca.* 1 μm) and uniform when the sample was doped at 35 °C for 6 h (Fig. 5a). The grains of iodine grew when either the doping time or temperature was increased (Fig. 5a–f). Notably, however, no iodine crystals were evident in the SEM images (Fig. 5g and h) of the iodine-doped 20NT/5CMK/$SQI_{0.1}$ (35 °C for 6 h). The presence of iodine in the SWNT/CMK-3/$SQI_{0.1}$ composite films was confirmed using Raman spectroscopy. After doping at 35 °C, doping times of 2, 6, 12, and 24 h caused the G-band to shift from 1572 cm^{-1} to 1575, 1577, 1581, and 1584 cm^{-1}, respectively (Fig. 6). The intercalation of polyiodide into the CNTs [30,31] would be consistent with this up-shift; intercalation of polyiodide presumably occurred in the 20NT/5CMK/$SQI_{0.1}$ composite films. Furthermore, a broad band (*ca.* 100–300 cm^{-1}) was featured in the Raman spectra after doping with iodine; this signal was attributed to the formation of charged I_3^- and

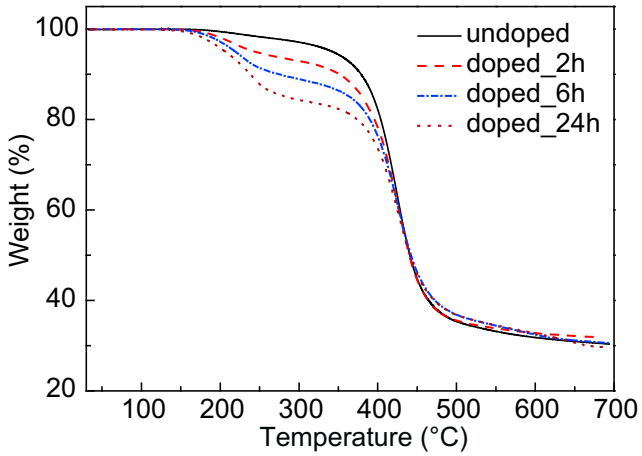

Fig. 7. Thermogravimetric curves of $SQI_{0.1}$ films doped under 35 °C for 0–24 h.

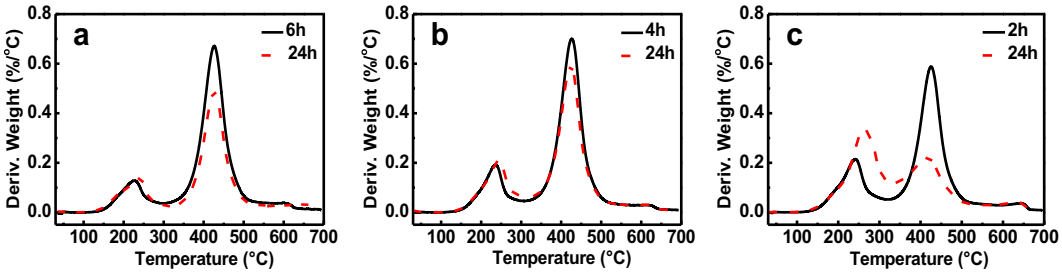

Fig. 8. The first derivative TGA curves of iodine-doped $SQI_{0.1}$ films doped under (a) 35 °C, (b) 40 °C and (c) 50 °C.

I_5^- polyiodide chains [30], the presence of which was also revealed in XPS spectra (Fig. S4, Table S1). From the SEM images and Raman spectra, it was concluded that iodine was dispersed well in the SWNT/CMK-3/$SQI_{0.1}$ composite films, presumably because of the great nanoporosity of CMK-3, which has been applied widely for nanodispersion in many fields [19,32–34].

3.3. *Influence of iodine-doping on stability and structure of polysquaraine ($SQI_{0.1}$)*

TGA was employed to determine the effect of iodine-doping on the stability of $SQI_{0.1}$ films that had been doped with iodine at 35 °C for 0–24 h (Fig. 7). Good thermal stability was exhibited by the pristine $SQI_{0.1}$ film, with the decomposition of the polymer backbone represented by a high decomposition *onset* temperature (385 °C) [8]. The weight losses of the iodine-doped $SQI_{0.1}$ films occurred at lower temperatures, between 150 and 330 °C, attributable to the elimination of free iodine and iodine centers [35]. For the $SQI_{0.1}$ films doped for 2, 6, and 24 h, the weight losses within the range 150–330 °C were 8.31, 12.33, and 16.68 wt.% respectively; these values are approximately equal to the mass fractions of doped iodine. Leaving the existence of iodine aside, the weight loss from backbone decomposition between 330 and 520 °C decreased when the doping time was increased from 2 to 6 to 24 h (62.14, 59.26, and 57.15 wt.%, respectively), hinting that the stability of the zwitterionic π-conjugated polymer $SQI_{0.1}$ was enhanced after doping with iodine.

To obtain more detailed understanding of the TGA data, TGA derivative curves of $SQI_{0.1}$ films doped at 35, 40, and 50 °C were recorded (Fig. 8); for simplicity, only the curves of the samples treated at optimized doping times (*i.e.*, 6 h at 35 °C, 4 h at 40 °C, and 2 h at 50 °C; refer to Fig. 3a) are displayed, as well as those of the corresponding specimens doped for 24 h. Two major peaks and one minor peak appeared in each of the derivative curves. The major peaks were attributable to the elimination of iodine (between 225 and 265 °C) and the decomposition of the polymer backbone (between 417 and 426 °C). The minor peak was evident in the trace of each of the iodine-doped $SQI_{0.1}$ films (between 600 and 650 °C; Fig. 8), but not in that of the pristine $SQI_{0.1}$ film (refer to Fig. S2). The existence of polyiodide intercalated in $SQI_{0.1}$ is suggested by this feature; similar phenomena have been reported previously [30,31,35]. Using XPS, the states of the intercalated polyiodide were characterized (Fig. S3); the $I_{3d5/2}$ spectra of the iodine-doped $SQI_{0.1}$ films prepared with different doping levels could be resolved into two peaks near 618 and 620 eV, which were attributable to the I_3^- and I_5^- anions, respectively. For simplicity, only the ratios of I_3^- and I_5^- for these specimens have been listed in Table 1. As the doping time increased, the iodine mass fraction increased, accompanied by an increase in the I_5^-/I_3^- ratio. The same trend appeared for the iodine-doped 20NT/5CMK/$SQI_{0.1}$ films (Table S1). A similar phenomenon has been observed in iodine-doped polyaniline [29]. These data also confirm that the small signals in the TGA derivative curves near 650 °C (Fig. 8) represent the existence of polyiodide intercalated in $SQI_{0.1}$.

To further understand the effect of polyiodide on the interchain packing structure, the XRD patterns of the $SQI_{0.1}$ films that had been doped at 35 °C were recorded. Feature peaks at values of 2θ of approximately 3.7, 19.6, and 26° appear in Fig. 9, corresponding to *d*-spacings of 23.9, 4.5, and 3.4 Å, which are associated with the interchain, interlayer, and interlayer π-stacking packing distances, respectively, of $SQI_{0.1}$ [8]. These three diffraction peaks were also present in the XRD patterns of all of the iodine-doped $SQI_{0.1}$ polymer films, but with values of 2θ that deviated slightly from those of the pristine film. In particular, the interchain packing distance increased pronouncedly from approximately 24 Å for the pristine

Table 1
Deconvolution data from $I_{3d_{5/2}}$ XPS spectra of SQI0.1 films doped with iodine at 35 °C for 0–24 h.

I_2-doped $SQI_{0.1}$	Binding energy (eV)	Percentage of total area (%)
2 h	618.28	59.5
	620.38	40.5
6 h	618.38	56.4
	620.08	43.6
12 h	618.28	55.5
	620.08	44.5
24 h	618.48	51.9
	620.28	48.1

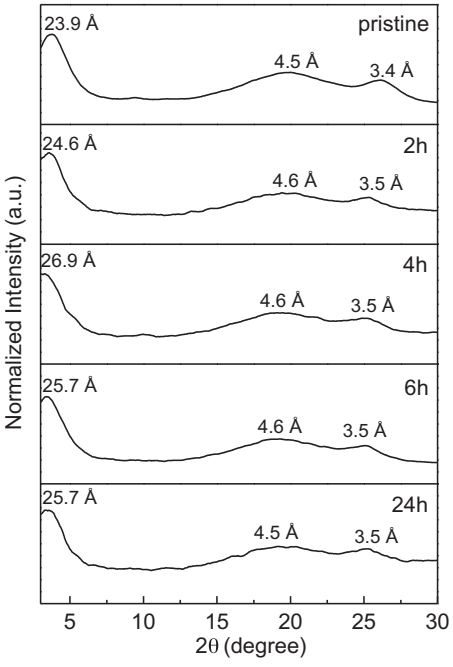

Fig. 9. XRD patterns of pristine iodine-doped $SQI_{0.1}$ films doped under 35 °C for 0–24 h.

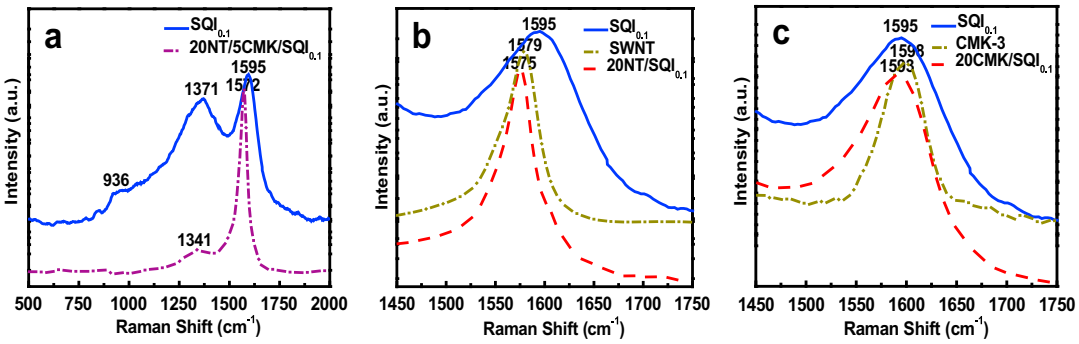

Fig. 10. Raman spectra of $SQI_{0.1}$ (a) 20NT/5CMK/$SQI_{0.1}$, (b) SWNT and 20NT/$SQI_{0.1}$ and (c) CMK-3 and 20CMK/$SQI_{0.1}$.

Table 2
Sample designations and the corresponding thermoelectric properties.

Sample	I_2-treatment	SWNT/CMK-3 (wt%)	σ (S cm^{-1})	S (μV K^{-1})	P (μW mK^{-2})	k (W mK^{-1})	ZT (at 300 K)
A	—*	—	2.589×10^{-5}	78.14	1.581×10^{-5}	0.325	1.458×10^{-8}
B-6	35 °C, 6 h	—	8.236×10^{-1}	133.84	1.475	0.139	3.175×10^{-3}
B-24	35 °C, 24 h	—	1.501×10^{-1}	105.69	1.677×10^{-1}	0.129	3.890×10^{-4}
C-4	40 °C, 4 h	—	8.816×10^{-1}	90.13	7.162×10^{-1}	0.239	8.967×10^{-4}
C-24	40 °C, 24 h	—	1.089×10^{-1}	61.34	4.097×10^{-2}	0.169	7.265×10^{-5}
D-2	50 °C, 2 h	—	6.446×10^{-2}	104.12	6.988×10^{-2}	0.158	1.325×10^{-4}
D-24	50 °C, 24 h	—	4.940×10^{-5}	95.17	4.474×10^{-5}	0.153	8.762×10^{-8}
E	—	20/0	3.586×10^{-2}	70.53	1.784×10^{-2}	0.351	1.523×10^{-5}
F	—	20/5	7.631×10^{-3}	66.58	3.383×10^{-3}	0.390	2.603×10^{-6}
E-6	35 °C, 6 h	20/0	5.264	43.45	9.939×10^{-1}	0.214	1.394×10^{-3}
F-6	35 °C, 6 h	20/5	7.162	63.16	2.86	0.351	2.444×10^{-3}
F-10	35 °C, 10 h	20/5	13.214	60.74	4.87	0.321	4.563×10^{-3}

*Pristine $SQI_{0.1}$.

film to approximately 27 Å after doping with iodine. Similar phenomena have been observed previously for the intercalation of iodine influencing the interchain packing distance [29]. Taken together, strong evidence is provided by these results for the existence of iodine in the chain structure of the polymer $SQI_{0.1}$.

3.4. π–π Interactions between carbon materials and polysquaraine ($SQI_{0.1}$)-based films

To examine the existence of π–π interactions between $SQI_{0.1}$-based films and the carbon materials, Raman spectra of the $SQI_{0.1}$ film, SWNT, CMK-3, 5CMK/$SQI_{0.1}$, 20NT/$SQI_{0.1}$, and 20NT/5CMK/$SQI_{0.1}$ were recorded (Fig. 10). Weak signals for C–O–C vibration of the polymeric side chain (936 cm^{-1}), C–C single bond stretching (1371 cm^{-1}), and C–C stretching of the benzenoid ring (1595 cm^{-1}) appear in the Raman spectrum of the $SQI_{0.1}$ film (Fig. 10a). In addition, the G-band (1572 cm^{-1}) of the 20NT/5CMK/$SQI_{0.1}$ composite film had shifted to lower frequency relative to those of the SWNTs (1579 cm^{-1}; Fig. 10b) and CMK-3 (1598 cm^{-1}; Fig. 10c). π–π Interactions between the SWNTs and the π-conjugated polymer were presumably responsible for this phenomenon [27,36,37]. In this present system, therefore, π–π interactions were suggested by the shift to exist between the $SQI_{0.1}$ matrix and the carbon materials (*i.e.*, SWNTs and CMK-3); these interactions were responsible for these carbon materials dispersing well in the $SQI_{0.1}$ matrix.

3.5. Thermoelectric properties of polysquaraine ($SQI_{0.1}$)-based films

The TE parameters of our $SQI_{0.1}$-based films are listed in Table 2; the Seebeck coefficient (S) of the pristine $SQI_{0.1}$ film (78 μV K^{-1}) was higher than those of other conjugated polymers [3,38,39]. In addition, the pristine $SQI_{0.1}$ film was a p-type TE material, as indicated by the positive Seebeck voltage. According to the definition of ZT, large σ/κ ratios are required for good TE materials. An increase in the value of σ has, however, always been accompanied previously by an increase in the value of κ; this behavior can be explained by the Wiedmann–Franz law [40]. Gratifyingly, this rule was not obeyed by the $SQI_{0.1}$ film developed herein when the value of σ was increased after doping with iodine. The values of σ and κ were improved (from 10^{-5} to 10^{-1} S cm^{-1}) and decreased (from 0.33 to 0.13 W mK^{-1}), respectively, after doping with iodine (until 6 h; Table 2). This special property was presumably derived from phonon scattering from the microstructure of the iodine-doped $SQI_{0.1}$ film (*vide supra*; SEM), the intercalation process (*vide supra*; TGA), and the variation of the interchain packing distance (*vide supra*; XRD), all of which led to lower overall values of κ. Accordingly, these materials appear to have great potential in TE applications. A suitable level of iodine-doping can simultaneously improve the value of σ significantly, enhance the value of S, and decrease the value of κ. For example, for the sample prepared under the optimized conditions (35 °C for 6 h), a power factor of 1.475 μW mK^{-2} and a value of ZT of 3.175×10^{-3} were obtained. Accordingly, these freestanding polysquaraine films have great potential for application in flexible thermoelectric devices. Finally, due to the π–π interaction between $SQI_{0.1}$ matrix and carbon materials, SWNTs and CMK-3 can greatly improve the flexibility of the composite film (Fig. 1) and the dispersion of the doped iodine (Fig. 5), respectively. Both are responsible for the enhancement of electrical conductivity. As the result, TE properties of the 20NT/5CMK/$SQI_{0.1}$ films doped for 10 h revealed a noticeable value of ZT of 4.563×10^{-3}, which is 143% of the optimized iodine-doped $SQI_{0.1}$ film, and 87% greater than that of the same sample that had been doped for 6 h.

4. Conclusions

A series of novel polysquaraine ($SQI_{0.1}$)-based films has been prepared and characterized; doping with iodine and integration of

SWNTs and CMK-3 enhanced the potential of these films for TE applications. The electrical conductivities (σ) of the $SQI_{0.1}$ films varied depending on the degree of iodine-doping, being optimized (8.816×10^{-1} S cm^{-1}) in the presence of 8–12 wt.% of iodine. In the case of the 20NT/5CMK/$SQI_{0.1}$ film, doping with iodine provided an excellent value of σ of 13.21 S cm^{-1}. According to TGA, XPS, and XRD analyses, the stability of the zwitterionic π-conjugated polymer $SQI_{0.1}$ improved after doping with iodine, with the resulting intercalated polyiodide influencing the interchain packing distance of the polymer. Signals for $\pi-\pi$ interactions between the carbon materials and the polymer $SQI_{0.1}$, a possible explanation for the high dispersion of the SWNTs and CMK-3 in the $SQI_{0.1}$ matrix, were evident in Raman spectra. Values of ZT of 2.603×10^{-6} and 4.563×10^{-3}, suitable for TE applications, were obtained after integration of carbon materials (*i.e.*, 20 wt.% SWNTs and 5 wt.% CMK-3) and further doping with iodine, respectively. For the iodine-doped 20NT/5CMK/$SQI_{0.1}$ film, the optimized value of ZT of 4.563×10^{-3} was 143% of the optimized iodine-doped $SQI_{0.1}$ film, revealing the great improvements that can result from increasing the doping time together with the integration of SWNT and porous carbon in $SQI_{0.1}$. The excellent dispersion of SWNTs in $SQI_{0.1}$ provides for other application opportunities.

Acknowledgment

We thank the National Science Council of the Republic of China, Taiwan, for supporting in this research financially under grants NSC100-2221-E009-023-MY3 and NSC 99-2221-E009-010-MY3 (W.-T. Whang) and 101-2218-E-035-005 (A.-Y. Lo).

Appendix A. Supplementary data

Supplementary data related to this article can be found at http://dx.doi.org/10.1016/j.matchemphys.2013.06.024.

References

[1] A.B. Kaiser, Phys. Rev. B 40 (1989) 2806.
[2] N.T. Kemp, A.B. Kaiser, C.J. Liu, B. Chapman, O. Mercier, A.M. Carr, H.J. Trodahl, R.G. Buckley, A.C. Partridge, J.Y. Lee, C.Y. Kim, A. Bartl, L. Dunsch, W.T. Smith, J.S. Shapiro, J. Polym, Sci., Part B: Polym. Phys. 37 (1999) 953.
[3] A. Shakouri, S. Li, Proceedings of International Conference on Thermoelectrics, 1999.
[4] X. Gao, K. Uehara, D.D. Klug, S. Patchkovskii, J.S. Tse, T.M. Tritt, Phys. Rev. B 72 (2005) 125202.
[5] J. Eldo, A. Ajayaghosh, Chem. Mater. 14 (2002) 410.
[6] A. Ajayaghosh, Acc. Chem. Res. 38 (2005) 449.
[7] H.C. Lu, W.T. Whang, B.M. Cheng, J. Mater. Chem. 21 (2011) 2568.
[8] M.C. Ho, C.H. Chao, C.H. Chen, R.J. Wu, W.T. Whang, Macromolecules 45 (2012) 3010.
[9] J.Y. Li, C.Y. Chen, C.P. Lee, S.C. Chen, T.H. Lin, H.H. Tsai, K.C. Ho, C.G. Wu, Org. Lett. 12 (2010) 5454.
[10] F.M. Silvestri, D. Irwin, L. Beverina, A. Facchetti, G.A. Pagani, T.J. Marks, J. Am. Chem. Soc. 130 (2008) 17640.
[11] C.J. Ko, Y.L. Chang, Y.N. Hsiao, P.L. Chen, S.H. Lin, W.T. Whang, K.Y. Hsu, M.H. Tsai, W.Y. Tsang, J. Mod. Optic. 58 (2011) 1215.
[12] J. Fabian, H. Nakazumi, M. Matsuoka, Chem. Rev. 92 (1992) 1197.
[13] J. Chen, X. Gui, Z. Wang, Z. Li, R. Xiang, K. Wang, D. Wu, X. Xia, Y. Zhou, Q. Wang, Z. Tang, L. Chen, Appl. Mater. Interfaces 4 (2012) 81.
[14] N. Grossiord, J. Loos, L. Laake, M. Maugey, C. Zakri, C.E. Koning, A.J. Hart, Adv. Funct. Mater. 18 (2008) 3226.
[15] C.K. Chiang, C.B. Fincher Jr., Y.W. Park, A.J. Heeger, Phys. Rev. Lett. 39 (1977) 1098.
[16] I. Lévesque, P.O. Bertrand, N. Blouin, M. Leclerc, G. Zotti, C.I. Ratcliffe, D.D. Klug, X. Gao, F. Gao, J.S. Tse, Chem. Mater 19 (2007) 2128.
[17] H. Shirakawa, E.J. Louis, A.G. MacDiarmid, C.K. Chiang, A.J. Heeger, J. Chem. Soc. Chem. Commun. (1977) 578.
[18] M. Choi, R. Ryoo, Nat. Mater. 2 (2003) 473.
[19] A.Y. Lo, C.T. Hung, N. Yu, C.T. Kuo, S.B. Liu, Appl. Energy 100 (2012) 66.
[20] H. Lu, J. Gou, Nanosci. Nanotechnol. Lett. 4 (2012) 1155.
[21] B.A. Arbuzov, Pure Appl. Chem. 9 (1964) 307.
[22] D. Zhao, J. Feng, Q. Huo, N. Melosh, G.H. Fredrickson, B.F. Chmelka, G.D. Stucky, Science 279 (1998) 548.
[23] S. Jun, S.H. Joo, R. Ryoo, M. Kruk, M. Jaroniec, Z. Liu, T. Ohsuna, O. Terasaki, J. Am. Chem. Soc. 122 (2000) 10712.
[24] R. Ryoo, S.H. Joo, M. Kruk, M. Jaroniec, Adv. Mater. 13 (2001) 677.
[25] P.R.L. Malenfant, J.M.J. Fréchet, Macromolecules 33 (2000) 3634.
[26] I.T. Kim, R.L. Elsenbaumer, Macromolecules 33 (2000) 6407.
[27] Q. Yao, L.D. Chen, W.Q. Zhang, S.C. Liufu, X.H. Chen, A.C.S. Nano 4 (2010) 2445.
[28] A.J. Heeger, J. Phys. Chem. B 105 (2001) 8475.
[29] X.R. Zeng, T.M. Ko, J. Polym. Sci. B 35 (1997) 1993.
[30] L. Grigorian, K.A. Williams, S. Fang, G.U. Sumanasekera, A.L. Loper, E.C. Dickey, S.J. Pennycook, P.C. Eklund, Phys. Rev. Lett. 80 (1998) 5560.
[31] W. Zhou, S. Xie, L. Sun, D. Tang, Y. Li, Z. Liu, L. Ci, X. Zou, G. Wang, Appl. Phys. Lett. 80 (2002) 2553.
[32] A.Y. Lo, S.B. Liu, C.T. Kuo, Nanoscale Res. Lett. 5 (2010) 1393.
[33] D.S. Dai, P. Zhou, J. An, H. Zheng, Key Eng. Mater. 519 (2012) 240.
[34] F. Kerdia, V. Capsb, A. Tuel, Micropor. Mesopor. Mater. 140 (2011) 89.
[35] F. Wang, Y.H. Lai, M.Y. Han, Macromolecules 37 (2004) 3222.
[36] J.E. Huang, X.H. Li, J.C. Xu, H.L. Li, Carbon 41 (2003) 2731.
[37] R.V. Salvatierra, M.M. Oliveira, A.J.G. Zarbin, Chem. Mater. 22 (2010) 5222.
[38] A.B. Kaiser, Adv. Mater. 13 (2001) 927.
[39] A.B. Kaiser, Rep. Prog. Phys. 64 (2001) 1.
[40] L. Miao, S. Tanemura, R. Huang, C.Y. Liu, C.M. Huang, G. Xu, A.C.S. Appl. Mater. Interfaces 2 (2010) 2355.